Title
Cross-sectional thermo-mechanical responses of energy piles

Authors
Moradshahi, Aria
Faizal, Mohammed
Bouazza, Abdelmalek
et al.

Publication Date
2021-10-01

DOI
10.1016/j.compgeo.2021.104320

Peer reviewed

Manuscript

Cross-Sectional Thermo-mechanical Responses of Energy Piles

Aria Moradshahi[1], Mohammed Faizal[2], Abdelmalek Bouazza[3*], John S. McCartney[4]

[1]PhD student, Monash University, Department of Civil Engineering, 23 College Walk, Clayton, Vic. 3800, Australia. Telephone: +61 3 990 58901; Email: aria.moradshahi@monash.edu

[2]Research Fellow, Monash University, Department of Civil Engineering, 23 College Walk, Clayton, Vic. 3800, Australia. Telephone: +61 3 9902 9988; Email: mohammed.faizal@monash.edu

[3*] (corresponding author), Professor, Monash University, Department of Civil Engineering, 23 College Walk, Clayton, Vic. 3800, Australia. Telephone: +61 3 9905 4956; Email: malek.bouazza@monash.edu

[4]Professor and Department Chair, University of California San Diego, Department of Structural Engineering, 9500 Gilman Drive, SME 442J, La Jolla, CA 92093-0085, USA, Telephone: +1 858 534 9630; Email: mccartney@ucsd.edu

Abstract

Despite the widespread research on energy piles, there remain critical knowledge gaps in the cross-sectional thermal responses of concrete energy piles. This paper implements a unique research approach by developing and validating a numerical model with cross-sectional temperatures and strains measured in a field-scale energy pile (diameter = 0.6 m and length = 10 m), strengthening the reliability of modelling for energy piles. The numerical model was further used to investigate the influences of inlet fluid temperature, soil thermal conductivity, soil elastic modulus, soil thermal expansion coefficient, and the presence of a nearby energy pile at a centre-to-centre distance of 3.5 m on the cross-sectional thermal responses of an energy pile. These investigations demonstrate the practical significance of the above parameters on the cross-sectional thermal responses of energy piles. The results show that the temperature and stresses were largest at the centre of the pile and reduced with increasing radial distance to the pile's edge, with differences up to 4°C and 2.2 MPa, respectively, between the centre and the edge. A comparison of the cross-sectional results with existing stress estimation methods,in the cross-section of the piles, commonly based on average cross-sectional temperature and temperature measured at a single spot, reveal that existing methods lead to an overdesign of 2 MPa. Therefore, the actual temperature and stress variations in the planar cross-section of energy piles should be accounted for in the design of energy piles.

Keywords: *Energy piles; field tests; cross-sectional thermal responses; soil property effects; fluid temperature effects.*

Introduction

It is well established that ground source heat pumps used in tandem with energy piles result in variations in temperature, deformations, and stress in the energy pile and surrounding soil. Due to the transient changes in the temperature of the heat pump circulating fluid, the temperature across an energy pile's cross-section will also vary (Abdelaziz and Ozudogru 2016a, 2016b; Caulk et al. 2016; Han and Yu 2020; Liu et al. 2020). However, the majority of field-scale studies on energy piles only measured their thermal response at a single location in the cross-section of the pile (e.g. Laloui et al. 2006; Bourne-Webb et al. 2009; Akrouch et al. 2014; Murphy et al. 2015; Murphy and McCartney 2015; Sutman et al. 2015; Faizal et al. 2016, 2018; Mimouni and Laloui 2015; Rotta Loria and Laloui 2017a, 2017b, 2018; Fang et al. 2020; Moradshahi et al., 2020a and b; Wu et al. 2020). Assuming that the temperature measured at the single location is representative of the temperature across the cross-section of an energy pile has been shown to lead to errors in estimating thermal strains and stresses, mostly when heating and cooling occur (McCartney et al. 2015; Murphy and McCartney 2015; Abdelaziz and Ozudogru 2016a, 2016b; Caulk et al. 2016).

Numerical studies showed that non-uniform temperature and stress variations occurred between the centre and edge of the energy pile (Abdelaziz and Ozudogru 2016a, 2016b; Caulk et al. 2016; Han and Yu 2020; Liu et al. 2020), but fewer field studies have been performed to validate these observations (e.g. Faizal et al. 2019a; 2019b). Although Faizal et al. (2019a, 2019b) reported that temperature and stress calculated using sensors at similar radial distances, they did not measure temperatures or thermal axial stresses near the pile-soil interface. The pile temperature at the edge of the pile would be expected to be similar to the soil temperature, hence leading potentially to temperature and stress gradients across the pile's diameter.

The numerical studies mentioned above were conducted for a single energy piles with a given inlet fluid temperatures and one set of soil properties. Thus, factors governing the distribution in temperature and stress across an energy pile's cross-section are not fully understood. Accordingly, there is currently a knowledge gap on the effects of inlet fluid temperatures, soil properties, and the presence of a nearby energy pile on the distribution of temperatures and stresses in the cross-section of energy piles. The magnitudes of thermal stresses in energy piles depend on the magnitudes of inlet fluid temperatures (e.g. You et al. 2014; Mimouni and Laloui 2015; Murphy and McCartney 2015; Faizal et al. 2016; Han and Yu 2020). A recent parametric study based on field investigations (Moradshahi et al. 2020b) showed that soil parameters (i.e. soil thermal conductivity, λ_{soil}, thermal expansion coefficient, α_{soil}, and elastic modulus, E_{soil}) could affect the axial thermal stresses at the centre of the energy pile. Hence, it can be hypothesised that thermal stresses in the energy pile's cross-section will also be influenced. Variations of λ_{soil} affect the heat transfer between the pile and the soil (Jeong et al. 2014; Salciarini et al. 2015, 2017; Guo et al. 2018; Sani et al. 2019; Moradshahi et al. 2020b) which can affect the pile-soil interface temperatures and hence the temperature and stress distribution in the cross-section. Variations in α_{soil} and E_{soil} affect the restrictions imposed by the soil on the thermal expansion and contraction of energy piles (Bodas Freitas et al. 2013; Bourne-Webb et al. 2015; Salciarini et al. 2015; Khosravi et al. 2016; Rotta Loria and Laloui 2017b; Salciarini et al. 2017; Moradshahi et al. 2020b), which in turn could influence the magnitudes of stresses developed in the cross-section of the energy pile. Moreover, the presence of a nearby energy pile can also influence the cross-sectional temperature and stress distributions of an energy pile due to possible thermal interaction between the piles through the soil.

This paper presents a study on cross-sectional thermal responses of a field-scale energy pile obtained experimentally and numerically using a coupled thermo-mechanical model. In particular, the influence of inlet fluid temperatures, soil properties (soil thermal conductivity, λ_{soil}, thermal expansion coefficient, α_{soil}, and elastic modulus, E_{soil}) and the presence of a nearby energy pile on the temperature and stress distribution in the cross-section of the energy pile are investigated and discussed.

Site description and experimental procedure

The experiments were conducted on two energy piles installed under a six-storey residential building. A schematic of the piles is shown in Figure 1. The site's soil profile is Brighton Group of materials, consisting of dense to very dense clayey sands (Barry-Macaulay et al., 2013; Singh et al., 2015; Faizal et al., 2018, 2019a, 2019b). The piles' diameter and length were 0.6 m and 10 m, respectively. The average compressive strength and modulus of elasticity of unreinforced concrete samples measured in the laboratory are 64 MPa and 34 GPa, respectively. The piles were spaced at a centre-to-centre distance of 3.5 m. Both piles had four HDPE pipe U-loops installed up to the piles' depth. One of the two piles (EP1) was instrumented with vibrating wire strain gauges (Model: Geokon-4200) at five depths, as shown in Figure 1. Each depth contained five axial VWGs (V1 to V5) installed in the planar cross-section of EP1. The axial strain gauge V5 was located near the centre of the pile and axial strain gauges V1 to V4 were located approximately 160 mm away from the pile's edge. These axial VWSGs across the piles' cross-section were used to achieve this paper's objectives. The ground temperatures were recorded using Type T thermocouples at two boreholes located between the two piles (Figure 1). A detailed description of the piles' instrumentation is given in Faizal et al. (2019a and 2019b).

Two heating and two cooling experiments were conducted on a single pile (EP1) and dual piles (EP1 + EP2). The inlet water temperatures and the ambient temperatures for all experiments are described in Figure 2 and Table 1. The fluid temperatures were recorded using Type T thermocouples. The ambient temperatures were obtained from a weather station located approximately 13 km away from the experimental site. The sudden increase in inlet fluid temperature on day 4 of the dual pile heating experiment, shown in Figure 2, was due to switching on an additional heating element to increase the inlet fluid temperature. The inlet fluid temperature trend for the dual pile cooling experiment was affected on Days 8 and 15 due to some heat pump's performance issues. More details of the experiments are given in Table 1. The temperature data for heating and cooling tests for the single and dual pile experiments were obtained from Faizal et al. (2019a) and Moradshahi et al. (2020b). These data sets were used to validate the numerical model and investigate the influence of different parameters on the cross-sectional temperatures and axial thermal strains and stresses of EP1.

Numerical modelling

A numerical study was performed to evaluate the cross-sectional behaviour of EP1 for varying inlet fluid temperatures and soil properties (i.e. soil elastic modulus, E_{soil}, thermal conductivity, λ_{soil}, and thermal expansion coefficient, α_{soil},) for single and dual pile experiments. A three-dimensional finite element model was developed and simulated using COMSOL Multiphysics software. The model was validated against field results. The 40 × 15 × 30 m^3 model, shown in Figure 3, consisted of 381980 tetrahedral, triangular, prismatic, linear and vertex elements from which 108388 and 53981 mesh elements describe EP1 and EP2, respectively.

The model geometry was developed based on the field piles' dimensions and boundary conditions. The soil block dimensions were selected based on a preliminary numerical analysis to avoid boundary effects on the simulated results. Each energy pile was connected to a separate 5 × 5 m slab with a thickness of 0.5 m. A working load of 1400 kN (Faizal et al. 2019) was applied to the surface of the slab overlying the two pile heads (on the axis of pile centre) to simulate the building loads. Roller boundary conditions were applied to the sides of the numerical model to allow vertical movements while movements at the base of the model were entirely restricted. The energy piles and the soil were assumed to be bonded together; hence no interface elements were assigned at the pile-soil interface. Similar assumptions were made in various numerical studies reported in the literature (e.g. Batini et al. 2015; Gawecka et al. 2017; Rotta Loria and Laloui 2017b, 2018; Salciarini 2017; Adinolfi et al. 2018) and in a recent study on the cross-sectional thermal response of energy piles by Liu et al. (2020). There was no groundwater encountered within the soil over the pile's length during installation, and the soil at the site was considered dry.

The numerical modelling was conducted under the following assumptions: (a) the energy piles and slabs were isotropic, elastic and incompressible under isothermal conditions; (b) the inertial effects of the solid skeleton were negligible, and the simulations represented quasi-static conditions; (c) the Mohr-Coulomb model governed by non-associated flow rules was used for modelling soil behaviour; and (d) the heat transfer between the piles and the ground was due to conduction. The material thermal and mechanical properties of the soil, energy piles, slab and the HDPE pipe, were adopted from previous studies conducted on the site (Barry-Macaulay et al. 2013; Singh et al. 2015; Faizal et al. 2018, 2019) and other studies reported in the literature (Bowles 1968; Peck et al. 1974; Mitchell and Soga 2005; Bourne-Webb et al. 2009; Amatya et al. 2012, Singh and Bouazza 2013).

Field results and numerical validation

The distribution of EP1 temperatures and axial thermal strains were obtained from the axial VWSGs located in the planar cross-section of EP1. The locations of these axial VWSGs, shown in Figure 1, were non-dimensionalised with respect to the radius of EP1. In this regard, the axial VWSG at location V5 (Figure 1) corresponds to the centre of EP1, V1 and V2 correspond to the non-dimensional radius of -0.47, and V3 and V4 correspond to the non-dimensional radius of 0.47. The axial thermal stresses in EP1 were estimated using the following equation:

$$\sigma_T = E_P(\varepsilon_{obs} - \alpha_{free}\Delta T) \quad (1)$$

where E_P is the elastic modulus of the concrete, ε_{obs} is experimentally observed thermal strains, α_{free} is the free thermal expansion coefficient of the concrete (taken as 13 με/°C), and ΔT is the change in temperature of the pile. Positive thermal strains indicate expansion and negative thermal stresses indicate compression.

The field and numerical results for Day 14 of each experiment along the cross-section of EP1 for the depths of 3.05 m (near the null point) and 7.28 m (representative of EP1 behaviour of lower parts of EP1) are shown in Figure 4. It should be noted that the numerical temperatures, thermal strains and stresses have been obtained from the same aforementioned experimental non-dimensional radius for the purpose of validation. There was a good match between experimental and numerical results, hence giving confidence in using the model for more detailed parametric investigations. A good match between experimental and numerical results was also obtained at other depths. The experimental and numerical results show a low range of variations of temperature (up to 1.5°C), strains (up to 26με) and stresses (up to 2 MPa) over the cross-section of EP1 for all experiments (Figures 4a and 4b). The overall trends and magnitudes of temperatures and axial thermal strains and stresses were similar in the single and dual pile experiments, indicating the negligible effect of the operation of EP2 on the cross-sectional thermal response of EP1.

The experimental and numerical transient ground temperature changes in Boreholes 1 and 2 (see Figure 1) for all four experiments are shown in Figure 5. There was a good match between experimental and numerical results. For single heating and cooling experiments, the ground temperature changes in BH1 is greater than that of BH2. However, in the dual pile experiments, the ground temperature changes in BH2 were higher than in the single pile experiments as a result of EP2 being heated or cooled.

Numerical investigation

A parametric evaluation was performed using the validated numerical model to investigate the effect of varying fluid temperature and varying λ_{soil}, E_{soil}, and α_{soil} on the cross-sectional thermal response of EP1. For each heating and cooling experiment, two inlet fluid temperatures were studied, as shown in Figure 6. The fluid temperatures were varied by ± 10°C intervals for heating and cooling operations (i.e. $|\Delta T_f|$ = 10°C, and 20°C, where ΔT_f is the difference between the inlet fluid temperatures at the end of the experiment and the initial fluid temperature of 20°C which is close to the average ground temperature). The intervals of $|\Delta T_f|$ = 10°C were chosen to perform the parametric analysis on the effect of soil properties on the thermal response of EP1 for both heating and cooling operations. Three different values of each soil parameter were investigated (i.e. $0.5\lambda_{soil}$, λ_{soil}, $2\lambda_{soil}$; $0.5E_{soil}$, E_{soil}, $2E_{soil}$; $0.1\alpha_{soil}$, α_{soil}, $10\alpha_{soil}$). The initial pile and ground temperatures, fluid flow rate and ambient temperatures were kept the same for all the simulations. The two energy piles were also not connected in series and worked separately with the same inlet fluid temperatures (shown in Figure 6) and the same fluid flow rate of 11 L/min.

Results and discussions

Thermal responses across different diametrical axes

The cross-sectional thermal response of EP1 over the four different axes (i.e. X-axis, Y-axis, D1-axis, and D2-axis, as shown in Figure 3d) at a depth of 2.5 m for $|\Delta T_f|$ = 10°C is shown in Figure 7. The depth of 2.5 m had the highest stresses compared to other depths, and is likely the null point's location. The magnitudes of temperatures and thermal strains/stresses were symmetrical between heating and cooling for a given axis. Higher values of temperature, thermal strains and stresses were observed at the centre of EP1 compared to the edge of EP1 for both single and dual pile tests. The change in temperature at the centre and edge of the pile were approximately ± 8.5°C and ± 6.9°C (difference of ~ 1.6°C), respectively, while the stresses were ± 1.7 MPa and ± 0.4 MPa (difference of ~ 1.3MPa), respectively. The pile temperature reduced to the magnitudes of ground temperatures at the pile-soil interface (discussed in the following sections). The strains and stresses varied along the cross-section due to variations in temperature distribution and variations in the pile's thermal expansion/contraction across the cross-section. The temperatures and strains/stresses are largest with almost constant magnitudes between R = – 0.14 m and R = 0.14 m since this region is enclosed by the evenly distributed thermally active heat exchanger loops. The reduction in temperatures and thermal strains/stresses between R = ± 0.14 m and the pile-soil interface, at R = ± 0.3 m, is due to the difference in temperatures between the heat exchanger loops and the ground.

The differences between the cross-sectional thermal response of EP1 for all different four axes is insignificant with the maximum difference of about 0.3°C, 7$\mu\varepsilon$, and 0.2 MPa for changes in pile temperature, thermal axial strains, and thermal axial stresses, respectively, for all operations. Therefore, the distribution of thermal responses in the cross-section can be considered similar across different diametrical axes of the pile. As there were no significant differences in the different axes' thermal responses, the X-axis in the following sections of the paper is chosen to investigate the cross-sectional thermal response of EP1 for varying soil parameters.

Fluid temperatures

The effect of varying inlet fluid temperatures on the cross-sectional thermal responses of EP1 at a depth of 2.5 m and adjacent ground temperature changes at the same depth are shown in Figure 8. The change in pile and ground temperatures and thermal strains/stresses increased with increasing fluid temperatures. The pile temperatures are largest at the centre of the pile (Figure 8a) and reduce to the value of ground temperatures at the pile-soil interface (Figure 8b). The two energy piles' operation simultaneously increased/decreased the change in ground temperatures between the two energy piles, compared to single pile operation for heating/cooling operation (Figure 8b). The ground temperature changes were higher during dual pile tests due to thermal interference between the soil volumes influenced by each energy pile.

The difference between the magnitude of temperature and axial thermal stresses between the centre and edge of EP1 increased from 1.6°C to 3.1°C and from 1.3 MPa to 2.1 MPa respectively, with increasing fluid temperature from $|\Delta T_f|$ of 10°C to 20°C. Liu et al. (2020) and Abdelaziz and Ozudogru (2016b) also reported differences of 1.5 MPa and 2 MPa, respectively, between the centre and the edge of the energy pile. Larger fluid temperatures during the operation of the GSHP will therefore induce higher differential temperatures and stresses in the cross-section of the piles. Even though the ground temperatures between the two energy piles were affected by the operation of EP2 in dual pile operation, the temperatures and thermal strains/strains developed in EP1 were similar for both single and dual pile operations. The negligible effects of EP2 on EP1 likely occurred due to minor changes in ground temperatures near the edge of EP1 (up to 0.3 m away from EP1 edge) for both single and dual pile operations. This indicates that the operation of EP2 did not have significant effects on the cross-sectional distribution of temperatures and thermal stresses of EP1. This can be related to the issue that a pile-cap does not connect the piles and that the piles are not close enough to cause any effects on the thermal responses of EP1 as a result of EP2 operation.

Soil thermal conductivity

The effect of soil thermal conductivity, λ_{soil}, on the cross-sectional thermal responses of EP1 and adjacent ground temperature changes at a depth of 2.5 m, for $|\Delta T_f|$ = 10℃, is shown in Figure 9. Symmetrical thermal responses were observed for heating and cooling operations for all λ_{soil} values. Higher λ_{soil} resulted in lower EP1 temperature changes. Higher λ_{soil} resulted in faster heat propagation in the soil, which resulted in lower thermal confinement around EP1, hence the pile temperatures were low. For a given λ_{soil}, the changes in ground temperature near EP1 is similar for both single and dual pile operations indicating that variation of λ_{soil} did not affect the temperature changes near EP1 edge for the pile spacing of this study. However, overlapping of the ground temperatures represents thermal interaction in the soil between the two piles between R = 0.6 m and 2.7 m for dual pile tests.

The stress variations at the centre of EP1 were insignificant compared to those at the edge of EP1 when λ_{soil} increased from $0.5\lambda_{soil}$ to $2\lambda_{soil}$. This can be related to the fact that the centre of EP1 is more influenced by the heat-exchanger loops, whereas the edges of EP1 is more affected by ground temperature changes at the pile-soil interface. As a result, the difference between thermal stresses at the centre and edge of EP1 increased from 0.8 MPa to 1.65 MPa when λ_{soil} increased from $0.5\lambda_{soil}$ to $2\lambda_{soil}$. The effect of operating EP2 in dual pile operation on EP1 temperature distribution, axial thermal strains and stresses were insignificant for all values of λ_{soil}, which indicates that thermal interaction between the two energy pile is insignificant in the current study.

Soil elastic modulus

The effect of soil elastic modulus, E_{soil}, on the cross-sectional thermal responses of EP1 and adjacent ground temperature changes at a depth of 2.5 m, for $|\Delta T_f|$=10℃, is shown in Figure 10. The thermal responses were symmetrical for heating and cooling. The pile and ground temperatures were not affected by varying E_{soil} (Figures 10a and b). The thermal stresses increased (and hence decrease in thermal strains) with increasing E_{soil}, which can be attributed to increased soil restriction on thermal expansion/contraction of EP1. Khosravi et al. (2016) and Moradshahi et al. (2020b) also reported an increase in pile thermal stresses with increasing E_{soil}.

The distribution of temperatures and thermal stresses and strains were similar over the cross-section of EP1 for both single and dual pile operation indicating that operation of EP2 in dual pile operation did not have significant effects on EP1 thermal responses for different values of E_{soil}. An increase of 1.5 MPa of thermal stresses was observed when E_{soil} increased from 0.5E_{soil} to 2E_{soil}. However, the difference between the thermal stresses between the centre and edge of EP1 remained approximately 1 MPa for any given E_{soil} for single and dual piles' heating and cooling operations.

Soil thermal expansion coefficient

Figure 11 shows the effect of soil's thermal expansion coefficient, α_{soil}, on the cross-sectional thermal responses of EP1 and adjacent ground temperature changes at a depth of 2.5 m, for $|\Delta T_f| = 10°C$. Similar to E_{soil} and λ_{soil}, the thermal responses of EP1 for heating and cooling operations were symmetrical for both single and dual pile operations. Variations of α_{soil} did not affect the pile and ground temperature changes (Figures 11a and 11b).

The range of thermal stresses for various magnitudes of α_{soil} was lower than that for E_{soil}. Similar to what was observed for λ_{soil} and E_{soil}, the distribution of thermal stresses in EP1 was similar for both single and dual pile operations, hence the operation of EP2 did not affect the thermal responses of EP1 for the pile spacing investigated in this study. The differences in thermal stresses between the centre and edge of EP1 were about 1 MPa for all values of α_{soil}, for both heating and cooling operations of single and dual piles. A reduction of thermal stresses resulted in higher values of α_{soil} (i.e., 10 α_{soil} which corresponds to a ratio of $\alpha_{soil}/\alpha_{pile}$ of 7) which can be attributed to greater soil expansion which resulted in lower soil restriction on EP1. Similar behaviour of thermal stresses was observed by Bourne-Webb et al. (2016) and Salciarini (2017) along the depth of an energy pile.

Comparison of cross-sectional thermal results against conventional energy pile analysis

The stress estimation in the cross-section of conventional energy piles is commonly done based on the average cross-sectional temperature or by measuring the temperature at a single location in the cross-section. A comparison between the cross-sectional results reported herein, and conventional energy pile analysis based on average and single point temperature and stress evaluations is shown in Figure 12. The comparisons are made for EP1 for single pile experiments only, for $|\Delta T_f|$=20℃, 2E_{soil}, 2λ_{soil}, and10α_{soil} (these showed maximum cross-sectional thermal responses as discussed earlier).

The single point analysis is taken at the centre of the pile; the magnitudes of the temperature at this location were used to calculate the thermal stresses using Equation 1 and were considered the same over the cross-section, as is done for conventional energy pile analysis. In the average temperature's analysis, the average temperature values over the cross section were used to calculate stresses using Equation 1, as is also done for conventional energy pile analysis. The results show significant differences in thermal responses between the current cross-sectional results and conventional methods. The single point analysis shows greater differences against the cross-sectional thermal responses results than the average magnitude's analysis.

The maximum differences in temperatures and stresses between the results reported in the current study and single point and average temperature analysis were 2 MPa and 1.5 MPa (3.5°C and 2.5°C), respectively, for $|\Delta T_f|$=20℃ (Figures 12a and 12b); 1.1 MPa and 0.55 MPa

(1.7°C and 1.4°C), respectively, for $2E_{soil}$ (Figures 12c and 12d); 1.5 MPa and 1.1 MPa (1.2°C and 0.8°C), respectively, for $2\lambda_{soil}$ (Figures 12e and 12f); and 1.1 MPa and 0.8 MPa (1.7°C and 1.4°C), respectively, for $2\alpha_{soil}$ (Figures 12g and 12h). These results indicate that considering the existing conventional methods may result in over design of energy piles.

Conclusions

This paper investigated the cross-sectional thermal response of one of two field-scale energy piles spaced at a centre-to-centre distance of 3.5 m under monotonic heating and cooling operations. A numerical model validated against field data was used to perform a parametric study to investigate the effects of varying inlet fluid temperatures, soil thermal conductivity, thermal expansion coefficient, and elastic modulus on the cross-sectional thermal response of the considered energy pile. The influences of the second energy pile on the temperatures and thermal stresses of the considered energy pile during dual pile operation were negligible for all fluid temperatures and soil parameters for the setting investigated in this study. However, the ground temperatures between the two energy piles during dual pile operation experienced larger changes than the operation of a single energy pile for all studied cases. The temperatures and stresses at the centre of the considered energy pile were larger compared to the edge of the pile, for all fluids and soil properties.

The soil elastic modulus effect was more significant on the cross-sectional thermal response of the considered energy pile compared to the soil thermal conductivity and soil thermal expansion. However, the soil thermal conductivity influenced the ground temperatures while the effects of soil elastic modulus and thermal expansion coefficient on ground temperatures were negligible. Variation of soil thermal conductivity mostly affected the magnitudes of thermal stresses at the edge of the considered energy pile due to variations in pile-soil interface temperatures. Comparing the numerical model results with the conventional approach to estimate the thermal stresses in the energy pile showed that the conventional methods might lead to overdesign of the energy piles.

This paper's outcomes show that only considering the thermal responses at the centre of energy piles might result in design errors as the temperatures and thermal stresses at the edge of the energy piles are lower than those at the centre of the energy pile. Moreover, the differences between the centre and edge of energy piles will differ for different fluid temperatures and soil properties encountered at different sites and should also be accounted for in energy pile designs.

References

Abdelaziz, S. L., and Ozudogru, T. Y. 2016a. Selection of the design temperature change for energy piles. Applied Thermal Engineering, 107, 1036–1045. https://doi.org/10.1016/j.applthermaleng.2016.07.067.

Abdelaziz, S., and Ozudogru, T. Y. 2016b. Non-uniform thermal strains and stresses in energy piles. Environmental Geotechnics, 3(4): 237-252. https://doi.org/10.1680/jenge.15.00032.

Akrouch, G., Sánchez, M., and Briaud, J-L. 2014. Thermo-mechanical behavior of energy piles in high plasticity clays. Acta Geotechnica, 9(3): 399-412. https://doi.org/10.1007/s11440-014-0312-5.

Amatya, B.L., Soga K., Bourne-Webb P.J. 2012. Thermo-mechanical behaviour of energy piles. Géotechnique, 62(6):503-519. https://doi.org/10.1680/geot.10.P.116.

Barry-Macaulay, D., Bouazza, A., Singh, R., Wang, B., and Ranjith, P. 2013. Thermal conductivity of soils and rocks from the Melbourne (Australia) region. Engineering Geology, 164: 131-138. https://doi.org/10.1016/j.enggeo.2013.06.014.

Bodas Freitas, T., Cruz Silva, F., and Bourne-Webb, P.J. 2013. The response of energy foundations under thermo-mechanical loading. In Proceedings of 18th international conference on soil mechanics and geotechnical engineering, 4: 3347-3350. Paris, France: Comité Français de Mécanique des Sols et de Géotechnique.

Bourne-Webb, P.J., B. Amatya, K. Soga, T. Amis, C. Davidson, and P. Payne. 2009. Energy pile test at Lambeth College, London: Geotechnical and thermodynamic aspects of pile response to heat cycles. Géotechnique, 59(3): 237–248. https://doi.org/10.1680/geot.2009.59.3.237.

Caulk, R., Ghazanfari, E., and McCartney, J.S. 2016. Parameterisation of a calibrated geothermal energy pile model. Geomechanics for Energy and the Environment, 5, 1–15. https://doi.org/10.1016/j.gete.2015.11.001.

Faizal, M., Bouazza, A., and Singh, R. M. 2016. An experimental investigation of the influence of intermittent and continuous operating modes on the thermal behaviour of a full scale geothermal energy pile. Geomechanics for Energy and the Environment, 8: 8-29. https://doi.org/10.1016/j.gete.2016.08.001.

Faizal, M., Bouazza, A., Haberfield, C., and McCartney J.S. 2018. Axial and radial thermal responses of a field-scale energy pile under monotonic and cyclic temperature changes. Journal of Geotechnical and Geoenvironmental Engineering, 144(10): 04018072. https://doi.org/10.1139/cgj-2018-0246.

Faizal, M., Bouazza, A., McCartney, J. S., and Haberfield, C. 2019a. Effects of cyclic temperature variations on thermal response of an energy pile under a residential building. Journal of Geotechnical and Geoenvironmental Engineering, 145(10): 04019066.

Faizal, M., Bouazza, A., McCartney, J.S., and Haberfield, C. 2019b. Axial and radial thermal responses of an energy pile under a 6-storey residential building. Canadian Geotechnical Journal, 56(7): 1019–1033. https://doi.org/10.1061/(ASCE)GT.1943-5606.0001952.

Fang, J., Kong, G., Meng, Y., Wang, L., and Yang, Q. 2020. Thermomechanical behavior of energy piles and interactions within energy pile–raft foundations. Journal of Geotechnical and Geoenvironmental Engineering, 146(9): 04020079. https://doi.org/10.1061/(ASCE)GT.1943-5606.0002333.

Guo, Y., Zhang, G., and Liu, S. 2018. Investigation on the thermal response of full-scale PHC energy pile and ground temperature in multi-layer strata. Applied Thermal Engineering, 143: 836–848. https://doi.org/10.1016/j.applthermaleng.2018.08.005.

Han, C., and Yu, X. B. 2020. Analyses of the thermo-hydro-mechanical responses of energy pile subjected to non-isothermal heat exchange condition. Renewable Energy. https://doi.org/10.1016/j.renene.2020.04.118.

Jeong, S., Lim, H., Lee, J.K., and Kim, J. 2014. Thermally induced mechanical response of energy piles in axially loaded pile groups. Applied Thermal Engineering, 71(1): 608-615. https://doi.org/10.1016/j.applthermaleng.2014.07.007.

Khosravi, A., Moradshahi, A., McCartney, J.S., and Kabiri, M. 2016. Numerical analysis of energy piles under different boundary conditions and thermal loading cycles. E3S Web Conference, 9: 05005. EDP Sciences.

Laloui, L., Nuth, M., and Vulliet, L. 2006. Experimental and numerical investigations of the behaviour of a heat exchanger pile. International Journal for Numerical and Analytical Methods in Geomechanics, 30(8): 763-781. https://doi.org/10.1002/nag.499.

Liu, R. Y. W., Taborda, D. M. G., Gawecka, K. A., Cui, W., and Potts, D. M. 2019. Computational study on the effects of boundary conditions on the modelled thermally induced axial stresses in thermo-active piles. In Proceedings of the XVII ECSMGE-2019.

McCartney, J. S., Murphy, K. D., and Henry, K. S. 2015. Response of an energy foundation to temperature fluctuations. In IFCEE 2015, (pp. 1691-1700).

Mimouni, T., and Laloui, L. 2015. Behaviour of a group of energy piles. Canadian Geotechnical Journal, 52(12): 1913-1929. https://doi.org/10.1139/cgj-2014-0403.

Mitchell, J.K. and Soga, K. 2005. Fundamentals of soil behavior, 3rd edition. Wiley, New Jersey.

Moradshahi, A., Khosravi, A., McCartney, J. S., and Bouazza, A. 2020b. Axial load transfer analyses of energy piles at a rock site. Geotechnical and Geological Engineering, **38**: 4711–4733. https://doi.org/10.1007/s10706-020-01322-5.

Moradshahi, A., Faizal, M., Bouazza, A., and McCartney, J. S. 2020b. Effect of nearby piles and soil properties on the thermal behaviour of a field-scale energy pile. Canadian Geotechnical Journal. 0(ja): -. https://doi.org/10.1139/cgj-2020-0353

Murphy, K.D., and McCartney, J.S. 2015. Seasonal response of energy foundations during building operation. Geotechnical and Geological Engineering, 33(2): 343-356. https://doi.org/10.1007/s10706-014-9802-3.

Peck, R. B., Hanson, W. E., and Thornburn, T. H. 1974. Foundation Engineering (2nd ed.). Wiley.

Rotta Loria, A.F. and Laloui, L. 2017a. The equivalent pier method for energy pile groups. Géotechnique, 67(8): 691–702. https://doi.org/10.1680/jgeot.16.P.139.

Rotta Loria, A.F. and Laloui, L. 2017b. Thermally induced group effects among energy piles. Géotechnique, 67(5): 374-393. https://doi.org/10.1680/jgeot.16.P.039.

Rotta Loria, A. F. and Laloui, L. 2018. Group action effects caused by various operating energy piles. Géotechnique, 68(9): 834-841. https://doi.org/10.1680/jgeot.17.P.213.

Sani, A.K., Singh, R.M., Tsuha, C., and Cavarretta, I. (2019). Pipe–pipe thermal interaction in a geothermal energy pile. Geothermics, 81: 209–223. https://doi.org/10.1016/j.geothermics.2019.05.004.

Rui, Y., and Soga, K. 2019. Thermo-hydro-mechanical coupling analysis of a thermal pile. Proceedings of the Institution of Civil Engineers-Geotechnical Engineering, 172(2), 155-173.

Saggu, R., and Chakraborty, T. 2016. Thermo-mechanical response of geothermal energy pile groups in sand. International Journal of Geomechanics, **16**(4): 04015100. https://doi.org/10.1061/(ASCE)GM.1943-5622.0000567.Salciarini, D., Ronchi, F., Cattoni, E., and Tamagnini, C. 2015. Thermo-mechanical effects induced by energy piles operation in a small piled raft. International Journal of Geomechanics, 15(2): 04014042. https://doi.org/10.1061/(ASCE)GM.1943-5622.0000375.

Salciarini, D., Ronchi, F., and Tamagnini, C. 2017. Thermo-hydro-mechanical response of a large piled raft equipped with energy piles: a parametric study. Acta Geotechnica, 12(4): 703-728. https://doi.org/10.1007/s11440-017-0551-3.

Singh, R. M. and Bouazza, A. 2013. Thermal conductivity of geosynthetics. Geotextiles and Geomembranes, 39, 1-8.

Singh, R. M., Bouazza, A., and Wang, B. 2015. Near-field ground thermal response to heating of a geothermal energy pile: Observations from a field test. Soils and Foundations, 55(6), 1412-1426.

Suryatriyastuti, M.E., Burlon, S., and Mroueh, H. 2016. On the understanding of cyclic interaction mechanisms in an energy pile group. International Journal for Numerical and Analytical Methods in Geomechanics, **40**(1): 3-24. https://doi.org/10.1002/nag.2382.

Sutman, M., Olgun, C. G., and Brettmann, T. 2015. Full-scale field testing of energy piles. In IFCEE 2015, (pp. 1638-1647).

You, S., Cheng, X., Guo, H., and Yao, Z. 2014. In-situ experimental study of heat exchange capacity of CFG pile geothermal exchangers. Energy and Buildings, 79: 23-31. https://doi.org/10.1016/j.enbuild.2014.04.021.

Wang, B., Bouazza, A., Singh, R.M., Haberfield, C., Barry-Macaulay, D., and Baycan, S., 2015. Posttemperature effects on shaft capacity of a full-scale geothermal energy pile. Journal of Geotechnical and Geoenvironmental Engineering, 141(4): 04014125. https://doi.org/10.1061/(ASCE)GT.1943-5606.0001266.

Wu, D., Liu, H., Kong, G., and Ng, C.W.W. (2020). Interactions of an energy pile with several traditional piles in a row. Journal of Geotechnical and Geoenvironmental Engineering, 146(4). https://doi.org/10.1061/(ASCE)GT.1943-5606.0002224.

Table 1. Details of energy pile experiments.

Operation mode	Description	Inlet water temperature (°C)	Inlet water flow rates (L/min)	Experiment duration (Days)	Ambient temperatures (°C)
Single heating	24 h of heating (Faizal et al. 2019a; Moradshahi et al. 2020)	46	11	18	12-25
Dual heating	24 h of heating (Moradshahi et al. 2020)	42	10	42	12-22
Single cooling	24 h of cooling	1	12	21	10-16
Dual cooling	24 h of cooling	5	10	14	15-23

Table 2. Material properties for numerical simulations calibrated against field test measurements.

Soil properties	Fill	Dense sand	Sandy clay	Sand	Pile	Slab	HDPE pipes
Depth, z (m)	0.0-0.5	0.5-3.5	3.5-6.0	6.0-12.5	1750	800	—
Elastic modulus, E (MPa)	15	600	75	120	35000	35000	—
Poisson's ratio, ν (—)	0.30	0.28	0.30	0.30	0.22	0.22	—
Total density, ρ (kg/m^3)	1750	1800	1950	2200	2200	850	—
Specific heat capacity, C_p (J/kg°C)	800	840	810	850	810	850	—
Thermal conductivity, λ (W/(m°C))	1.1	1.7	2.0	2.3	1.5	1.5	0.4
Linear coefficient of thermal expansion, α (με/°C)	10	10	10	10	13	13	—
Friction angle (degrees)	30	38	32	35	—	—	—
Apparent cohesion (kPa)	1	0.1	0.2	0.1	—	—	—

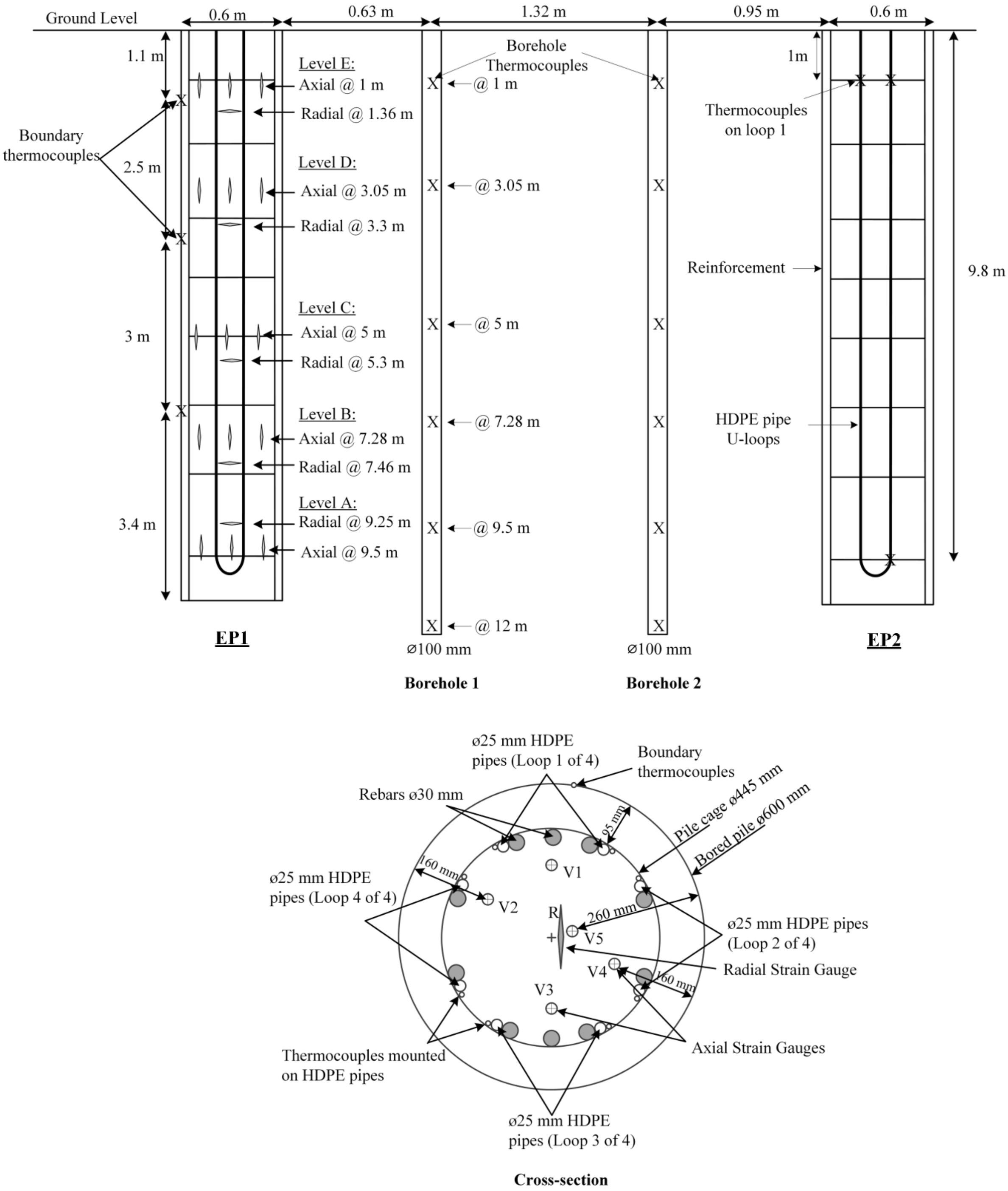

Figure 1. Field-scale energy piles details (after Faizal et al. 2018).

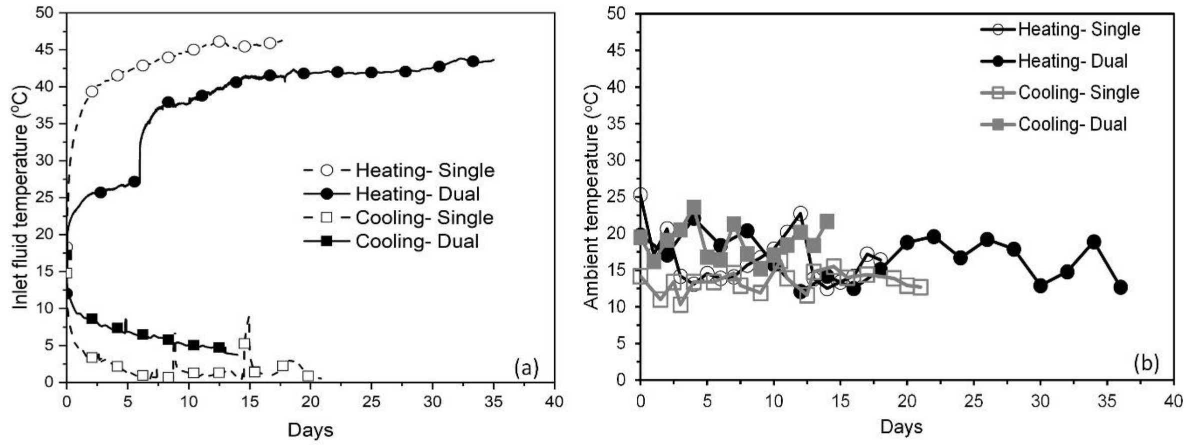

Figure 2. Temperatures for single and dual pile heating and cooling experiments (a) fluid temperatures; and (b) ambient.

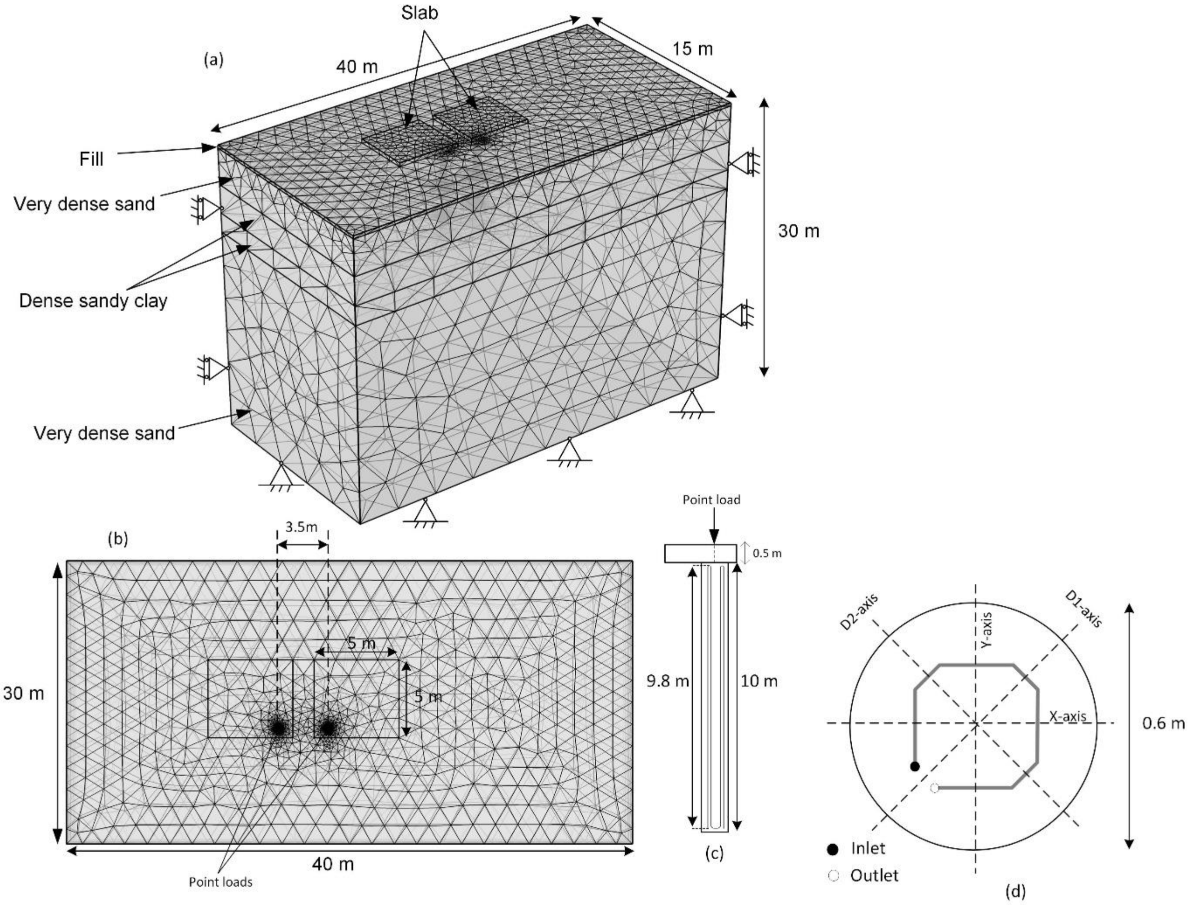

Figure 3. Finite element mesh of the numerical model (a) 3D view; (b) plan view; (c) side view of energy pile and heat exchanger loops; (d) plan view of energy pile, heat exchanger loops, and cross-sectional axes.

571

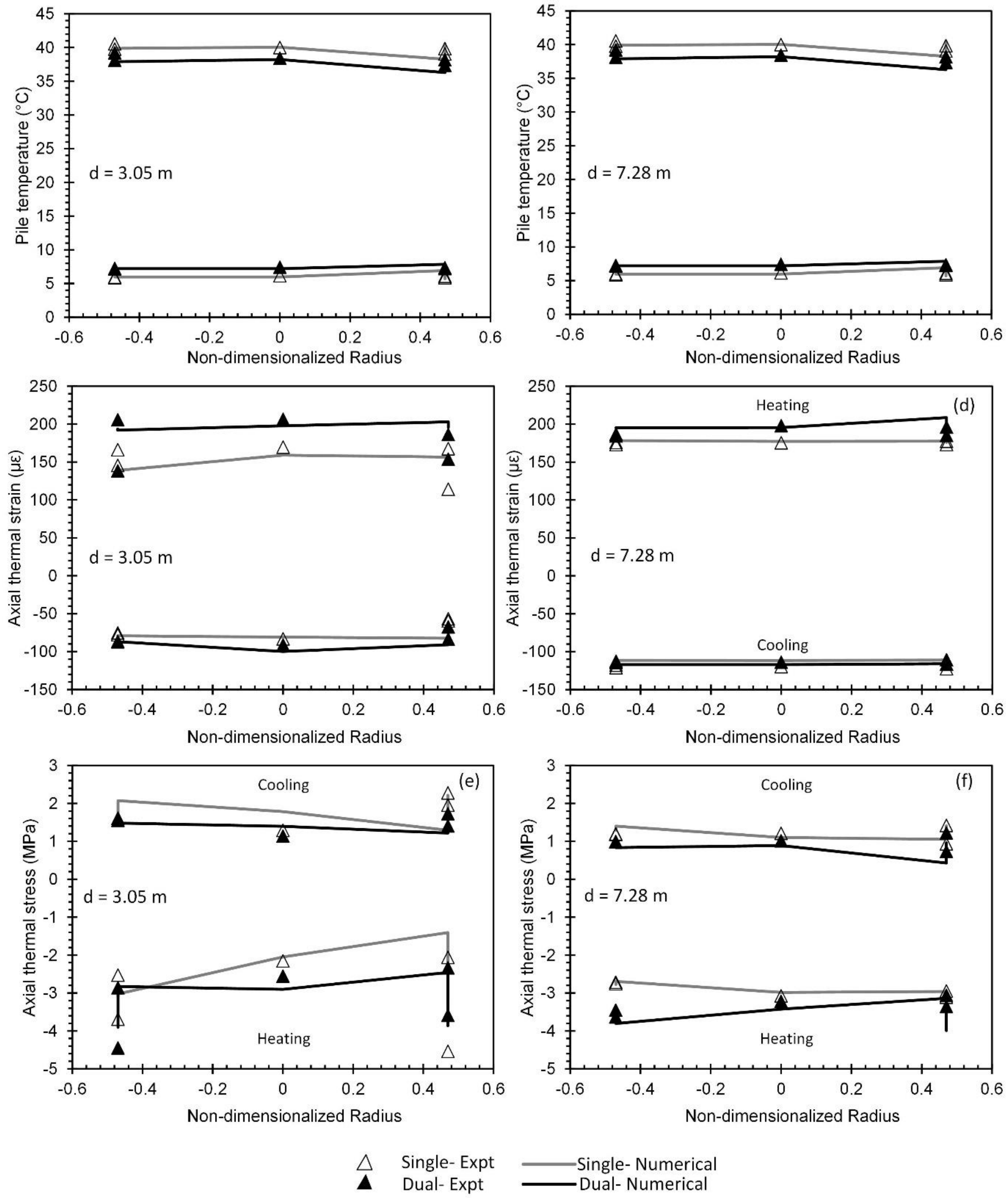

572 **Figure 4.** Field experimental and numerical cross-sectional distribution of thermal responses for EP1
573 at the end of Day 14: (a) and (b) temperatures at depths of 3.05 m and 7.28 m, respectively; (c) and (d)
574 axial thermal strains at depths of 3.05 m and 7.28 m, respectively; and (e) and (f) axial thermal stresses
575 at depths of 3.05 m and 7.28 m, respectively.

576

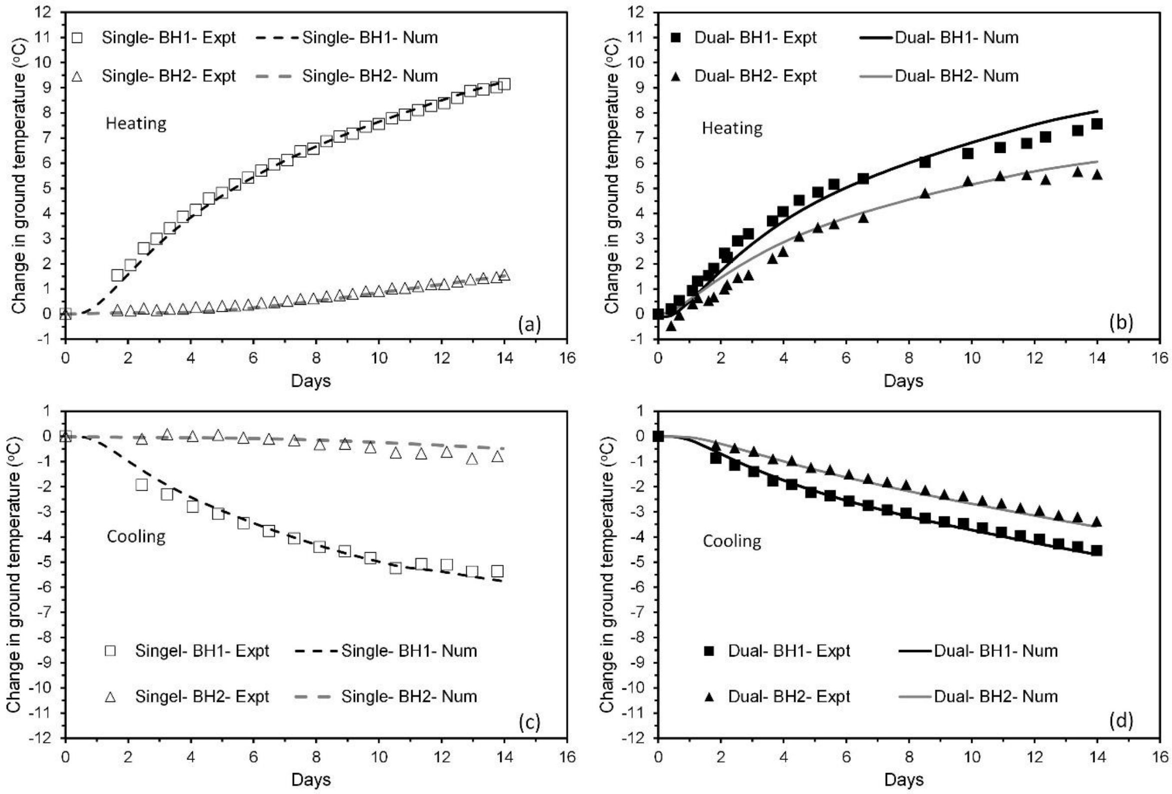

Figure 5. Field experimental and numerical change in ground temperatures: (a) for single pile heating operation; (b) for dual pile heating operation; (c) for single pile cooling operation; and (d) for dual pile cooling operation at depth of 2.5 m.

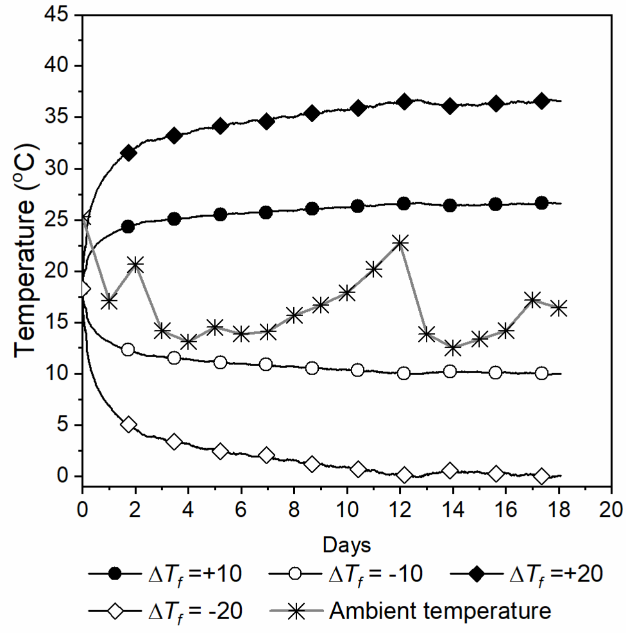

Figure 6. Inlet fluid variations considered in the parametric evaluations along with the ambient surface temperature variation.

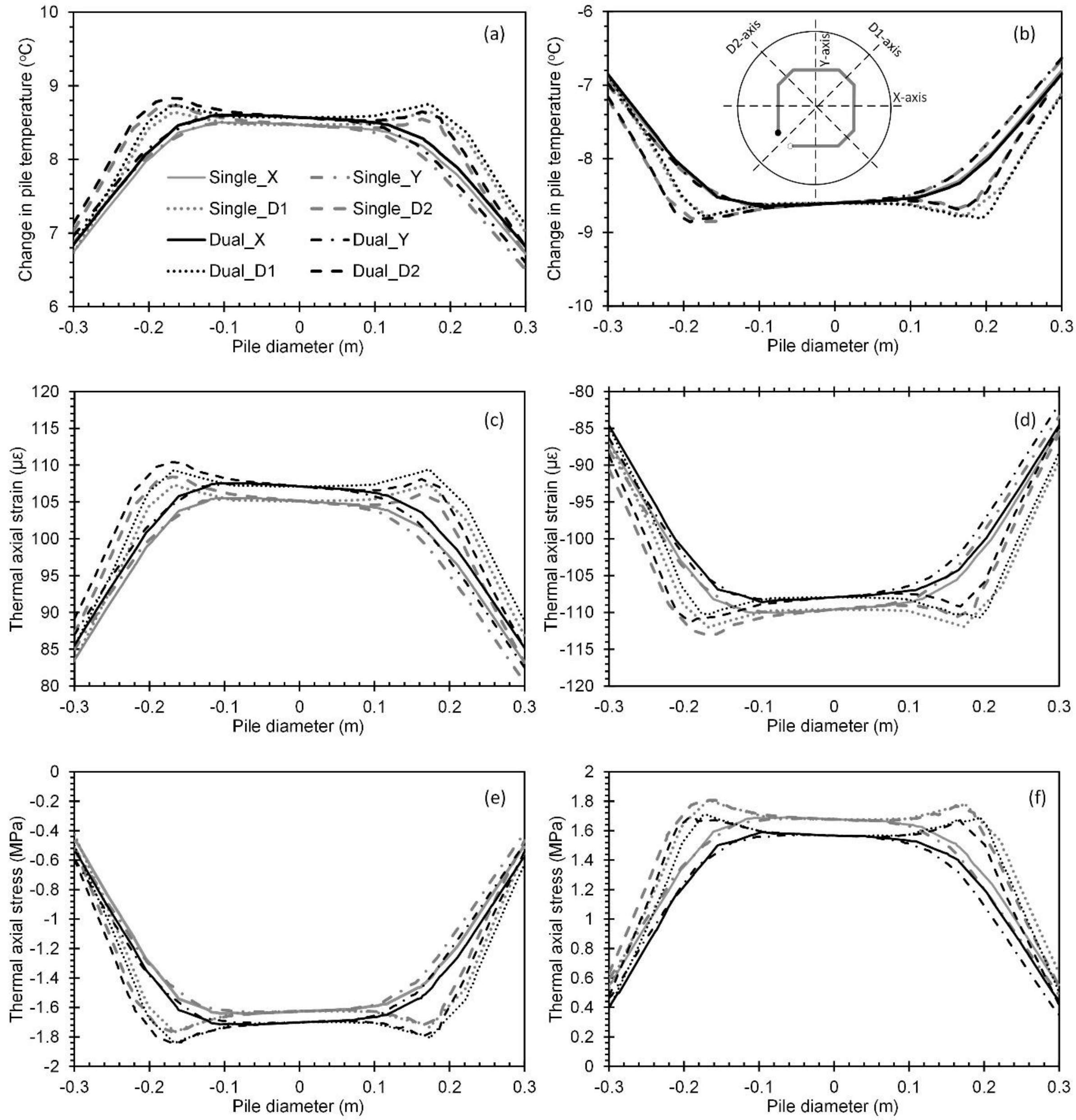

Figure 7. Numerical predictions of cross-sectional thermal responses of EP1 over different axes (shown in (b): (a) and (b) change in temperature during heating and cooling, respectively; (c) and (d) axial thermal strains during heating and cooling, respectively; and (e) and (f) axial thermal stresses during heating and cooling.

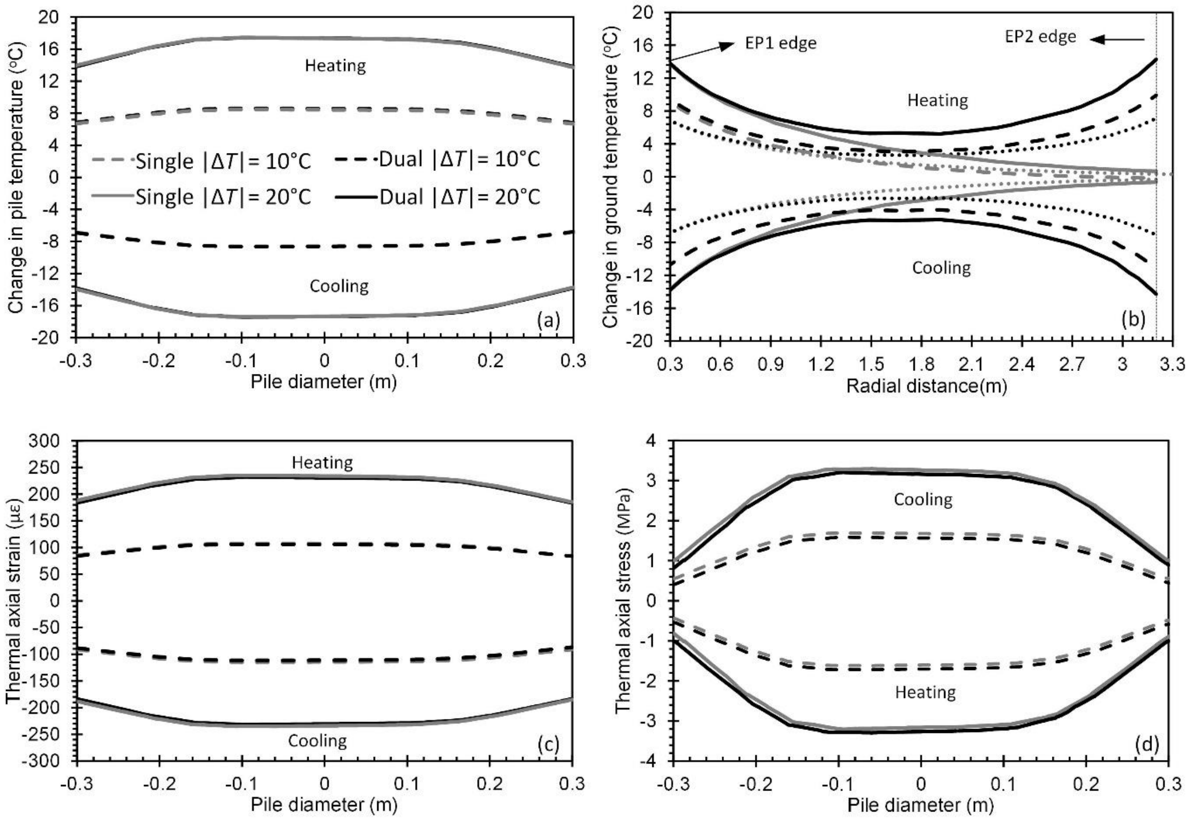

Figure 8. Numerical predictions of the effect of fluid temperature changes on the cross-sectional thermal responses of EP1 and ground temperatures: (a) change in pile's temperature; (b) change in radial distribution of ground temperatures; (c) thermal axial strains; and (d) thermal axial stresses in EP1.

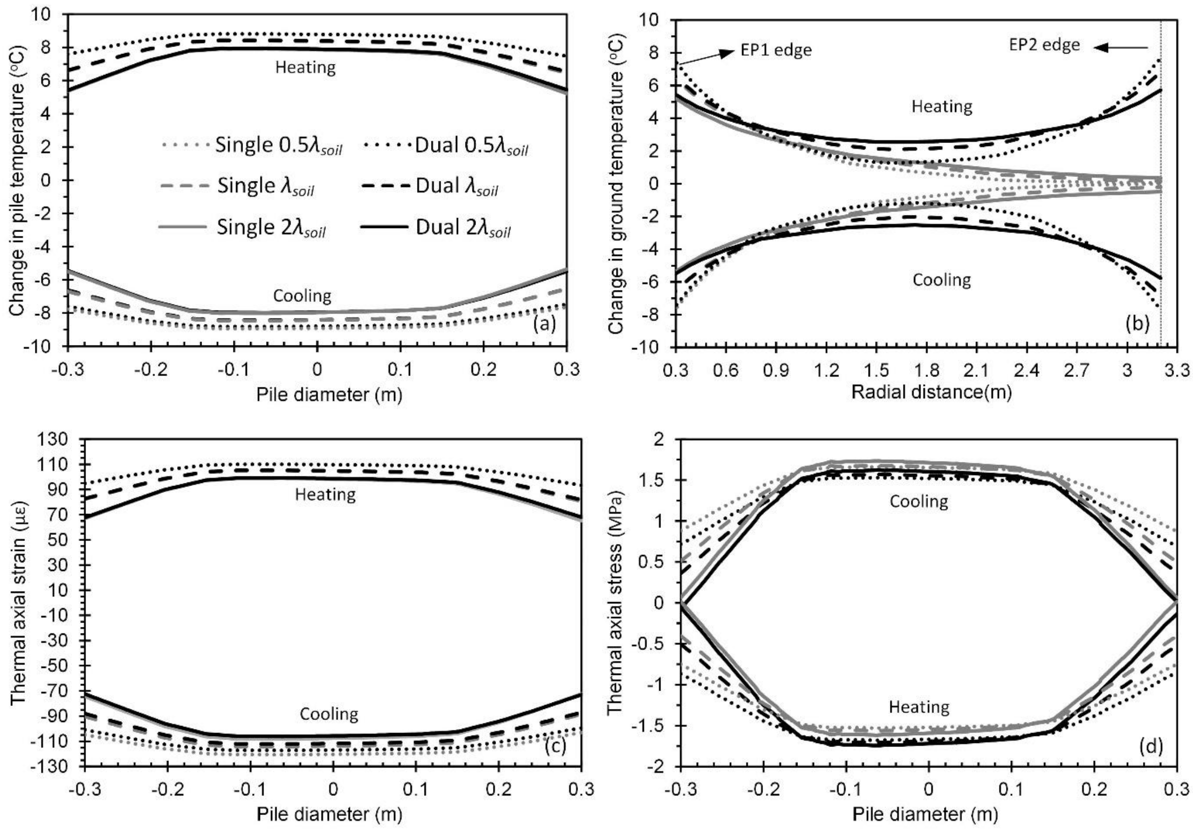

Figure 9. Numerical predictions of the effect of soil thermal conductivity, λ_{soil}, on the cross-sectional thermal responses of EP1 and ground temperatures: (a) change in pile's temperature; (b) change in radial distribution of ground temperatures; (c) thermal axial strains; and (d) thermal axial stresses.

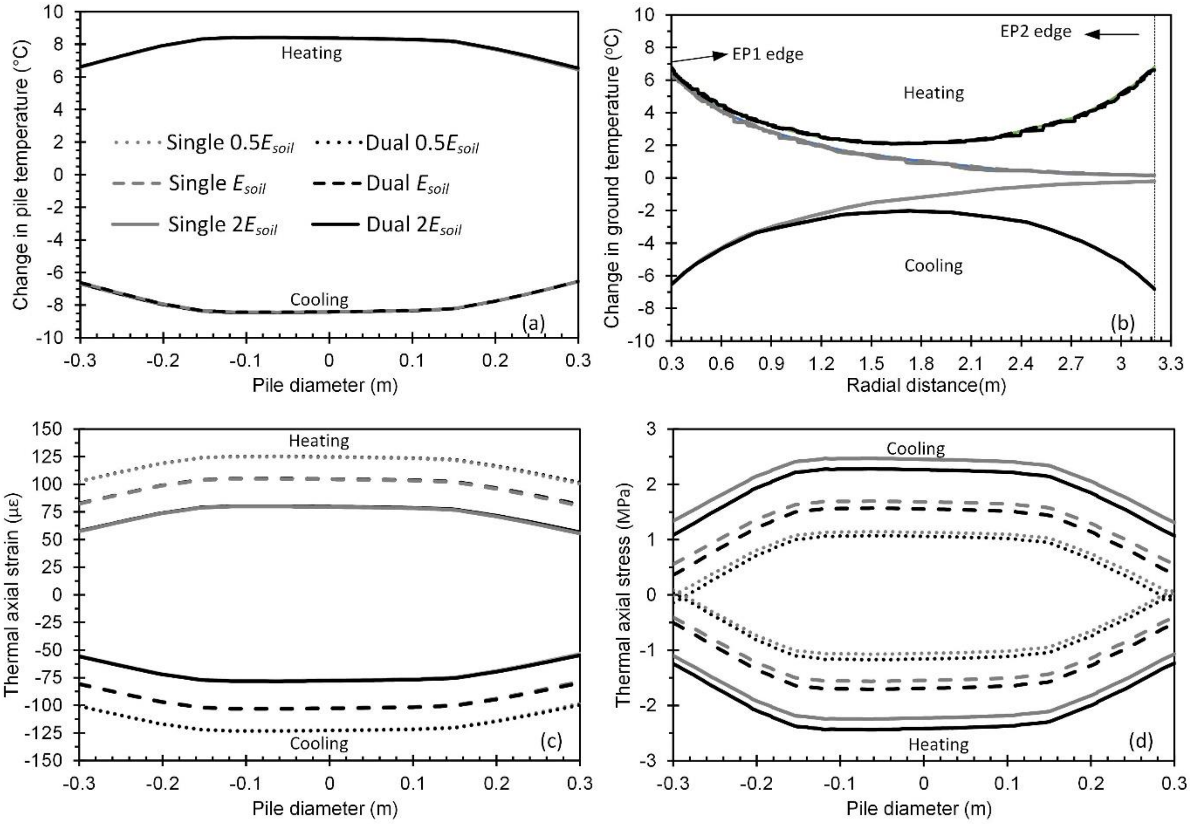

Figure 10. Numerical predictions of the effect of soil elastic modulus, E_{soil}, on the cross-sectional thermal responses of EP1 and ground temperatures: (a) change in pile's temperature; (b) change in radial distribution of ground temperatures; (c) thermal axial strains; and (d) thermal axial stresses.

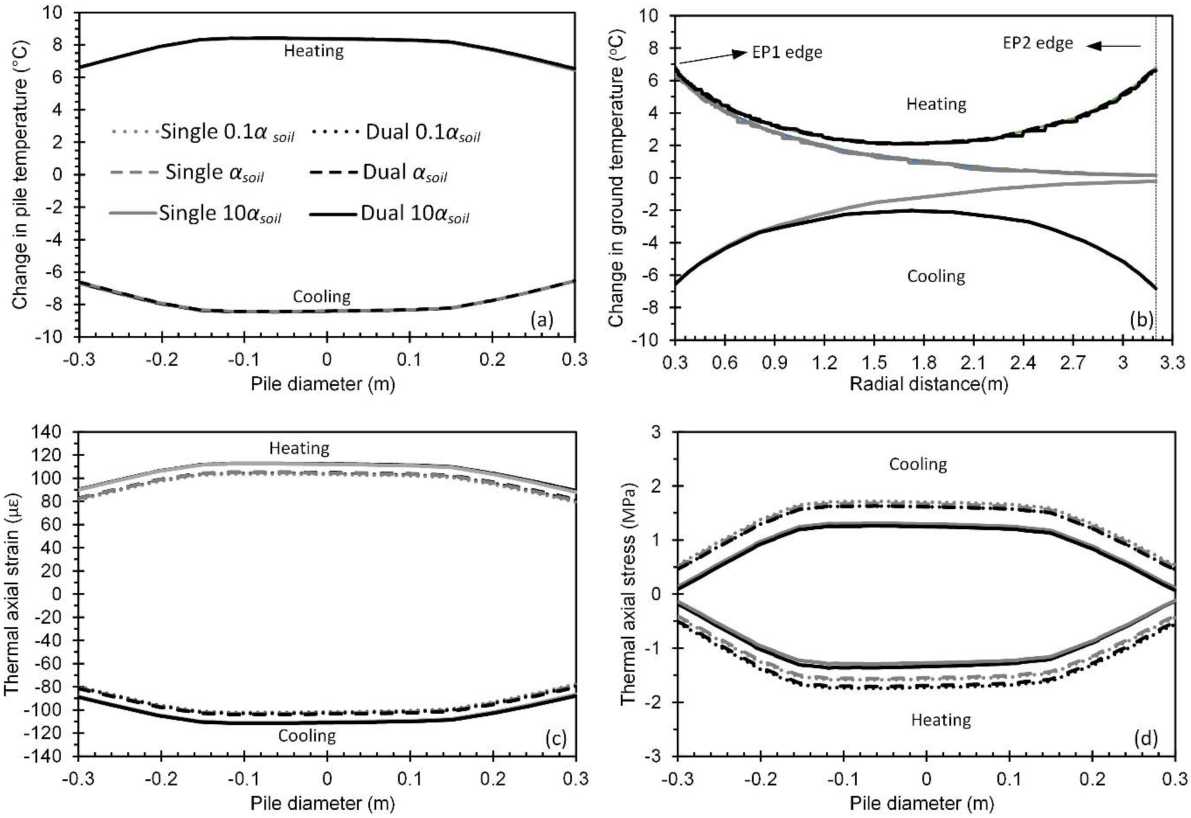

Figure 11. Numerical predictions of the effect of soil thermal expansion coefficient, α_{soil}, on the cross-sectional thermal responses of EP1 and ground temperatures: (a) change in pile's temperature; (b) change in radial distribution of ground temperatures; (c) thermal axial strains; and (d) thermal axial stresses.

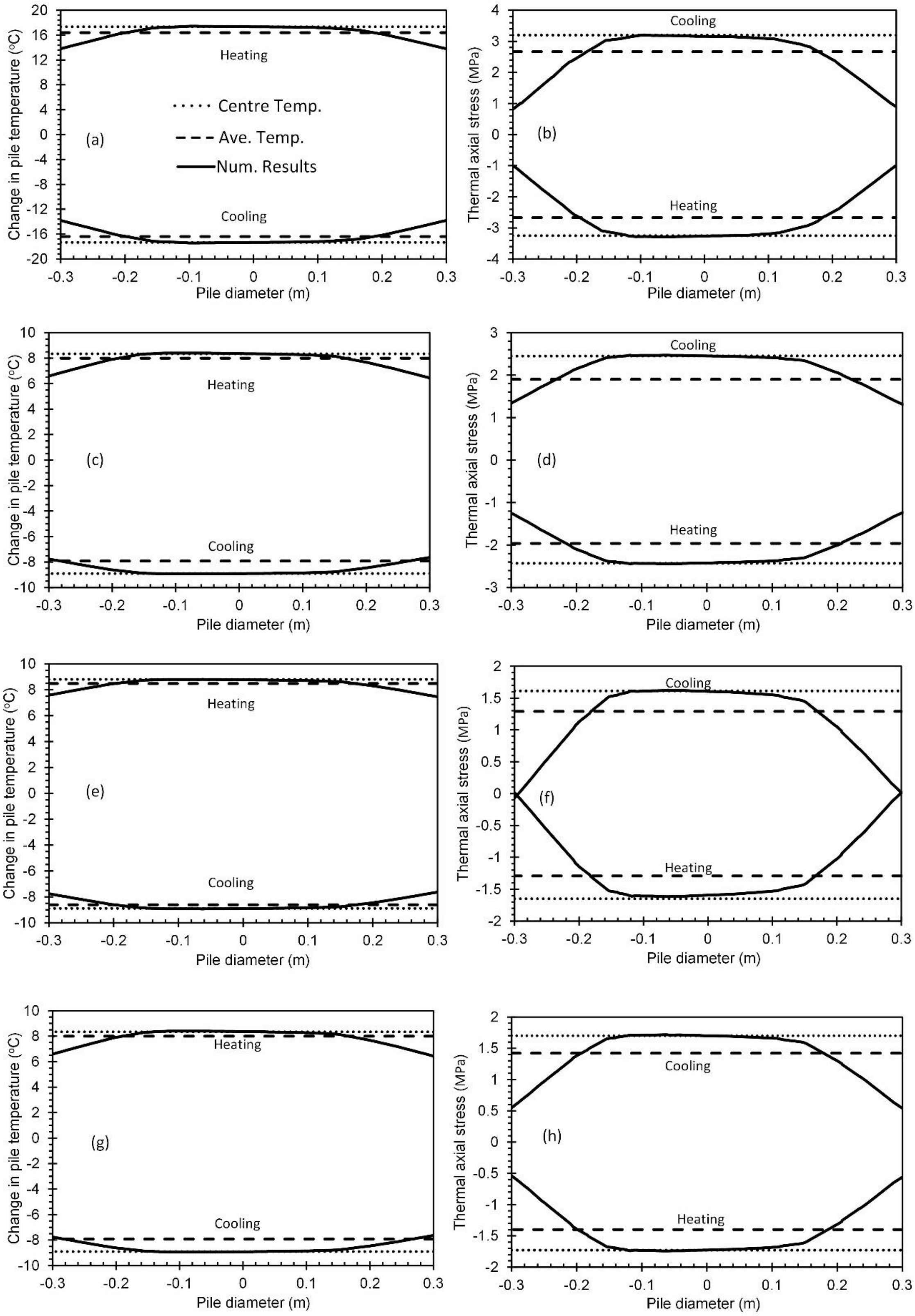

Figure 12. Comparison of the cross-sectional thermal responses of EP1 against temperature and stress distribution at a single location (centre) and average values for: a) and b) temperature and stress for ΔT = 20°C, respectively, c) and d) temperature and stress for $2E_{soil}$, respectively; e) and f) temperature and stress for $2\lambda_{soil}$, respectively; and g) and h) temperature and stress for $2\alpha_{soil}$, respectively.